

# A Comparison of the Temperature Dependence of Charge Recombination in the Ion-Radical Pair $P870^+Q_A^-$ and Tryptophan Fluorescence in the Photosynthetic Reaction Centers of *Rhodobacter sphaeroides*

P. P. Knox, E. P. Lukashev, B. N. Korvatovskii, V. V. Gorokhov, N. P. Grishanova, N. Kh. Seyfullina, V. Z. Paschenko\*, and A. B. Rubin

Department of Biology, Moscow State University, Moscow, 119991 Russia

\*e-mail: vz.paschenko@gmail.com

Received April 28, 2016

**Abstract**—The temperature dependences of the charge-recombination rate in the ion-radical pair  $P870^+Q_A^-$  in photosynthetic reaction centers of *Rhodobacter sphaeroides* were investigated. Recombination kinetics were measured in the individual absorption bands of the donor (600 nm) and an electron acceptor (335 and 420–450 nm) for the reaction center in the water–glycerol and trehalose environment after freezing preparations to  $-180^\circ\text{C}$  in the dark and on the actinic light and after their subsequent heating. In similar conditions the fluorescence lifetime of tryptophan in reaction centers ( $\lambda_{\text{reg}} = 325$  and  $345$  nm), which is an internal indicator of the dynamic state of the protein matrix, was measured. A correlation between the temperature dependences of functional and dynamic parameters of reaction centers in different solvents was shown. The differences in the average fluorescence lifetime of tryptophan in reaction centers of preparations frozen in the dark or on the actinic light were found. These results are explained due to transitions of reaction centers between different conformational states and processes of proton relaxation in the structure of the hydrogen bonds in the environment of reaction-center cofactors.

**Keywords:** pigment–protein complex, reaction center, primary quinone acceptor, bacteriochlorophyll, tryptophan, ion-radical charge recombination, conformational states

DOI: 10.1134/S0006350916060191

## INTRODUCTION

The pigment–protein complexes of photosynthetic reaction centers (RCs) are actually a photoactive enzyme in which its conformational dynamics plays a crucial role during all stages of the conversion of light energy, including in the temporary stabilization of electrons in the acceptor part of the RC [1–5]. Effective electrostatic stabilization of electrons on the  $Q_A$  and  $Q_B$  quinone acceptors in RCs of the pheophytin-quinone type significantly slow the process of dark recombination of separated charges associated with displacements of protons in their protein environment. As was shown for the RC of purple bacteria, the binding of  $H^+$  when semiquinones occur in the RC is not a diffusely controlled process; it is regulated by changes associated with conformational transitions between “available” and “unavailable” states prior to the actual binding or transfer of  $H^+$  in the RC structure [6]. Our previous comparative study of the kinetics of redox

conversions of the primary electron donor (dimer of bacteriochlorophyll P) in the RC structure of the purple bacteria *Rb. sphaeroides* and the final quinone  $Q_B$  electron acceptor in their individual absorption bands in the course of a one-electron reversible charge transfer between P and  $Q_B$  demonstrated that the kinetics of the dark recombination of the electron from  $Q_B^-$  to  $P^+$  that was recorded in the  $Q_B$  absorption bands (335 nm and 420–450 nm) was slower than the kinetics recorded in the  $Q_x$ -absorption band P (600 nm) [7]. We explained this by the relaxation processes in the environment of the  $Q_B$  associated with electrostatic stabilization of the electron transferred to  $Q_B$  due to displacement of protons in hydrogen bonds of the protein environment of the RC. The activation energy ( $U_a$ ) and the characteristic time ( $\tau_r$ ) of this process were equal to  $U_a = 1.2$  kcal/mol ( $= 0.052$  eV) and  $\tau_r = 0.1$  s for RCs in the water–buffer environment at physiological temperatures. The relatively small value of activation energy compared with the thermal energy and higher relaxation time value, according to the

Abbreviation: RC, reaction centers.

molecular scale, indicate the specific mechanism of the relaxation process due to displacements of protons and deformation of hydrogen bonds of the  $Q_B$  environment. Important information about the relationship of the electron-transport activity of the RC and its intramolecular dynamics was provided by experiments on the freezing of the RC to cryogenic temperatures in the dark or on activating light in different solvents followed by a parallel study of the temperature dependences of the functional and dynamic values of RC preparations during heating. Previously, this type of research allowed us to confirm our hypotheses about conformational changes in the RC associated with the electron transfer that regulate the basic constants of this transfer, in particular, during changes of temperature [3, 8].

The fluorescence of tryptophanyl residues in proteins is an informative internal natural indicator of the conformation of proteins, as well as their dynamics and intra/intermolecular interactions. It is known that the fluorescence of indole chromophore is highly sensitive to the state of its environment, including hydrogen bonds, and their responds to even small changes in its environment [9]. If the structure of a protein is known, then changes of tryptophanyl can be interpreted in terms of structural changes of the level of atomic resolution. The maximum position of the fluorescence of tryptophanyl residues in proteins, which is depends on the relaxation characteristics of the polar environment of the excited chromophore, has been used for many years as an indicator of the intramolecular dynamics of a protein, including the state during variation of the temperature [10]. The interpretation of the effects of the environment on the duration of the fluorescence of tryptophanyl residues in proteins is more complex. However, in recent years, an informative approach that associates the lifetime of excited tryptophanyl with the environment, including hydrogen bonds, has been developed [11].

The goal of this study was investigation and comparison of the temperature dependences of the electron-transport activity of reaction centers of *Rb. sphaeroides*, the dark recombination of the separated charges  $P^+$  and  $Q_A^-$ , measured in the individual absorption bands of the donor and acceptor of an electron, and the fluorescence characteristics of tryptophan fluorescence in RC samples that are frozen to cryogenic temperatures in the dark or on activating light in various solvents during their subsequent heating.

## MATERIALS AND METHODS

The study was carried out on RC preparations of the purple bacteria *Rhodobacter sphaeroides*. Bacterial cells were disrupted using an ultrasonicator. Chromatophores, separated by centrifugation were incubated for 30 min at 4°C in 0.01 M sodium phosphate

buffer at pH 7.0 that contained 0.5% zwitterionic detergent lauryldimethylamine oxide. They were then centrifuged at 144000 g for 90 min at 4°C. The RC fraction in the supernatant was separated by column chromatography on hydroxyapatite as described in [12]. The concentration of the obtained RC suspended in 0.01 M sodium phosphate buffer at pH 7.0, 0.05% lauryldimethylamine oxide was approximately 50  $\mu$ M.

Photo-induced reactions were investigated on a differential single-beam spectrophotometer with double monochromatization of the measuring light constructed at the Department of Biophysics, Faculty of Biology of Moscow State University. Laser Nd-YAG LS-2131M (532 nm, 8 ns, 5 mJ, LOTIS-TII, Belarus) was used as a source of light excitation. Photo-induced absorption changes were recorded at 600 nm ( $Q_x$  absorption band of P) and in the bands that reflect the redox conversion of ubiquinones of RCs at 335 nm and at 420–450 nm. The kinetics of the absorption changes at 335 nm and 420–450 nm were practically the same. However, since the amplitude of the signal at 450 nm was highest, redox transformations of ubiquinones of RCs were illustrated according to the results of measurements at this wavelength. The accumulation and averaging of 8–10 signals were performed for the improvement of the signal/noise ratio using an Octopus CS 8327 analog-to-digital converter (GaGe, the United States). The approximation of the obtained kinetic curves was performed using the ORIGIN software package. In experiments that involved freezing on the light, the sample (in the presence of o-phenanthroline at a concentration of  $10^{-2}$  M for blocking an electron transfer from  $Q_A$  to  $Q_B$ ) at room temperature was illuminated with white light using an incandescent lamp of the KGM type (350 W). When the light was on, the temperature was decreased to  $-180^\circ\text{C}$  within 10 min. The light was then switched off and the laser-induced absorption changes were measured. The temperature of the sample was then increased in the dark at increments of 10 degrees/min and photo-induced changes of absorbance were recorded.

Measurements of the protein-fluorescence spectra of the RC samples ( $\lambda_{\text{ex}} = 280$  nm) in the temperature range from  $-180$  to  $+35^\circ\text{C}$  were carried out using a Hitachi 850 (Japan) computerized spectrofluorimeter equipped with a cryostat constructed in the laboratory.

The measurement of the protein fluorescence lifetime of the RC was conducted on a Simple Tau 140 device operating in the photon counting mode (Becker & Hickl, Germany). The sample was placed in a liquid nitrogen-cooled cuvette, whose temperature was controlled using a thermocouple. In this case, the cooling time to  $-180^\circ\text{C}$  was approximately 10 min and the heating rate was  $5\text{--}7^\circ\text{C}/\text{min}$ . Upon cooling, the RC was activated with continuous light in the visible range with an intensity of approximately  $1\text{ W}/\text{cm}^2$ . At  $-180^\circ\text{C}$  the activating light was switched off. The flu-

orescence of the sample was excited at 280 nm using an EPLED 280 picosecond semiconductor laser (Edinburg Photonics, Ireland); the pulse duration was 870 ps, of the spectral width 10 nm, the pulse repetition rate was 1 MHz. The fluorescence was recorded using a K5900 16-channel multianode photomultiplier (Hamamatsu, Japan), in front of which a grating polychromator (600 grooves/mm) was located. The width of the spectrum at the output of the polychromator was 200 nm, which corresponded to 12.5 nm/channel. The integration time was 30 s. Thus, we obtained the three-dimensional ( $\lambda$ ,  $t$ ,  $I$ —intensity) picture of the fluorescence of tryptophanlys and we could registered the kinetics of the fluorescence decay at any point of the spectrum within 200 nm. Kinetic fluorescence curves were processed using the SPImage program (Becker & Hickl, Germany); the best approximation of the model curve with the experimental results was achieved by the two-exponential approximation. The average lifetime ( $\tau_{av}$ ) was calculated as the sum of the products of the amplitude on time of the corresponding two kinetic components.

## RESULTS AND DISCUSSION

During the cooling of RCs *Rb. sphaeroides* in the dark under conditions of high oxidative potential of the medium, when reversible electron transfer between the primary electron donor in the RC (dimer of bacteriochlorophyll P) and the  $Q_A$  and  $Q_B$  quinone acceptors occurs (electron transfer from  $Q_A$  to  $Q_B$  was almost completely inhibited at  $-30$ – $40^\circ\text{C}$ ) blocking of the direct electron transfer from  $Q_A$  to  $Q_B$  occurs. The rate of charge recombination between  $Q_A^-$  and  $P^+$  after light activation of samples frozen to  $-180^\circ\text{C}$  is 25–30 ms. At room temperature, the reaction time is substantially higher; approximately 100 ms. At room temperature and at  $-180^\circ\text{C}$  the kinetics of the recombination are approximated well by a single exponential. However, when samples frozen to  $-180^\circ\text{C}$  in the dark were heated, the kinetics of the recombination in the domain between the cryogenic and room temperatures became essentially non-exponential. A different pattern was observed for measurements of the kinetics of the recombination in RC samples cooled on the activating light. Under these conditions, the time of dark charge recombination of the  $P^+$  and  $Q_A^-$  remained close to that at room temperature (i.e., approximately 100 ms). Upon subsequent defrosting to  $-110^\circ\text{C}$ , a slight decrease in this time was observed, while further heating increased the time to values typical for room temperature. These results are explained by light induced transitions of RCs between different conformational substates, modulated by the temperature factor [5, 13].

In our experiments, we did not observe a difference in the rate constant of  $P^+$  and  $Q_A^-$  recombination in RCs containing 70% glycerol during heating of RCs

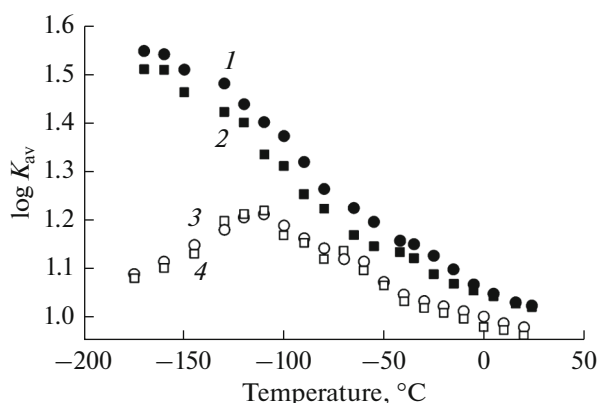


**Fig. 1.** The temperature dependence of the average recombination rate constant  $\log K_{av}$  of  $P^+$  and  $Q_A^-$  in RC *Rb. sphaeroides* (1, 3) and RC with isotopic substitution of  $H_2O$  to  $D_2O$  (2, 4) containing 70% glycerol and cooled to  $-180^\circ\text{C}$  in the dark (1, 2) or on the activating light (3, 4). Redox-conversions of RC were recorded in the 600 nm-band (1, 3) and at 450 nm (2, 4).

frozen in the dark by kinetic measurements at 450 and 600 nm in the entire range of temperatures. Therefore, in the presence of 70% glycerol in the domain from  $-180^\circ\text{C}$  to room temperature, the process of the recombination of  $P^+$  and  $Q_A^-$  is different from the above-discussed process of recombination of  $P^+$  and  $Q_B^-$ . The inability to experimentally observe differences for  $P^+$  and  $Q_A^-$  recombination for measurements in the range of 600 nm (the reduction of  $P^+$ ) and 450 nm (oxidation of  $Q_A^-$ ), was probably associated with a faster (by an order of magnitude) rate of this reaction compared to the recombination rate of  $P^+$  and  $Q_B^-$ . However, in RCs with isotope replacement of  $H_2O$  by  $D_2O$  we observed a slower kinetics of recombination of  $P^+$  and  $Q_A^-$  at 450 nm than in RC– $H_2O$  (Fig. 1). This difference in dark-adapted RC is especially significant at temperatures below  $-50^\circ\text{C}$ . Obviously, this fact, as is the case with  $Q_B$ , reflects the participation of H (D) atoms in redox-transformation and stabilization of an electron on  $Q_A$ .

The nonmonotonicity of these curves with a maximum at approximately  $-110^\circ\text{C}$  was characteristic for samples that were frozen in the light for both  $H_2O$ –RC and  $D_2O$ –RC: an increase in the recombination rate constant in the range from  $-180^\circ\text{C}$  ( $11\text{ s}^{-1}$ ) to  $-110^\circ\text{C}$  ( $12.5\text{ s}^{-1}$ ), followed by a decrease to  $10\text{ s}^{-1}$  at  $20^\circ\text{C}$  was observed (Fig. 1). The figure shows that in  $H_2O$ –RC and  $D_2O$ –RC we did not observe a significant difference between the values of the recombination rate constant obtained in the bands of 450 and 600 nm. We assume that in RCs frozen in the light the state with protons (deuterons) that were already “relaxed and frozen” at low temperature was probably formed under the effect of the light.

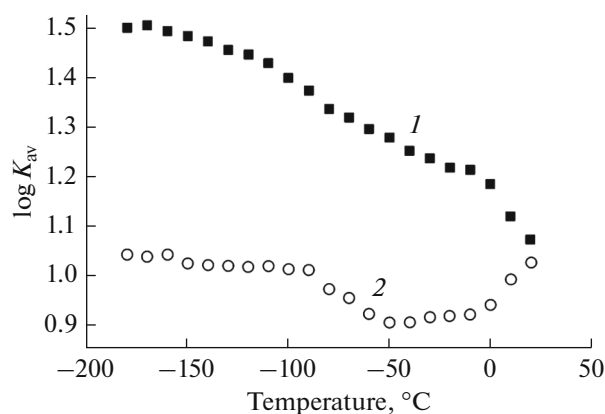


**Fig. 2.** The temperature dependences of the average recombination rate constant  $\log K_{av}$  of charges  $P^+$  and  $Q_A^-$  in RC of *Rb. sphaeroides*, containing trehalose and cooled to  $-180^\circ\text{C}$  in the dark (1) or on the activating light (2). Redox-conversions of RC were recorded in the 600 nm band.

For the vitreous RC sample with trehalose prepared according to [14] as a film on a glass surface the temperature profiles of the recombination rate dependence were significantly different from those for RCs in glycerol for both cooling in the dark or on the light (Fig. 2). The latter is probably due to changes in the structural and dynamic state of the environment of redox cofactors in RC structure with solvent replacement. This suggestion is confirmed by analysis of our fluorescence data.

The fluorescence spectrum of RC samples in 70% glycerol (Fig. 3, curve 3) at room temperature is approximated well by the sum of two Gaussian curves  $A1$  and  $A2$ , the first of which has a maximum at 327 nm and a half width of 35 nm, while the second is characterized by a maximum at 367 nm and a half-width of 88 nm. The ratio of areas was  $A2/A1 \approx 0.3$ . According to [10, 15], the  $A1$  component of the spectrum can be attributed to the fluorescence of tryptophan residues located inside the protein globule, which have relaxing polar groups (so-called class I) in their environment. The second component of the spectrum ( $A2$ ) assigned to the fluorescence of tryptophan residues which are replaced on the protein surface and are surrounded by bound water (class II). It should be noted that the contribution of tyrosine residues to the total protein fluorescence of RCs is insignificant, since the content of tryptophan residues in RC is 1.5 times higher than the content of tyrosine residues, in addition the ratio of tryptophan/tyrosine extinction coefficients  $\approx 5$  at a wavelength of 280 nm. Moreover, the quantum yield of tyrosine fluorescence in proteins is very low due to different quenching effects, including the formation of a hydrogen bond between the phenyl hydroxyl and the nearest ionized carboxyl group, as well also due to the transfer of electronic excitation energy to tryptophan molecules [16]. Studies con-

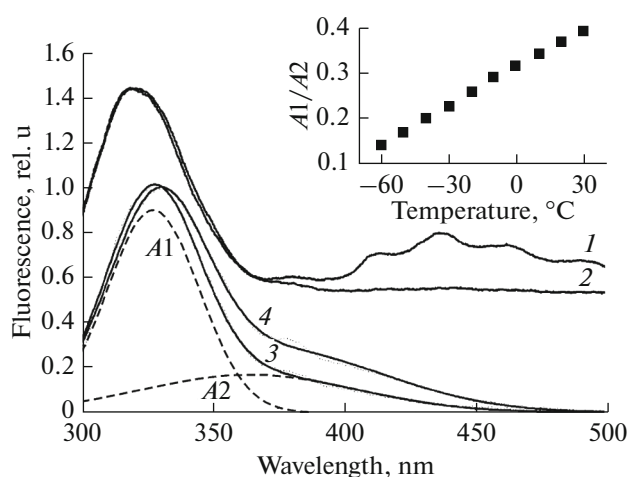


**Fig. 3.** The fluorescence spectra of RC of *Rb. sphaeroides* in 70% glycerol (1–3) and trehalose (4) at  $-180^\circ\text{C}$  (1),  $-70^\circ\text{C}$  (2) and room temperature (3 and 4), and the decomposition on the spectrum into Gaussian components ( $A1$  and  $A2$ ). The inset shows the ratio of the areas  $A2/A1$  for RCs in glycerol versus the temperature. Spectra are normalized to the maximum at 320–330 nm. For clarity, the curves 1 and 2 were shifted relatively to the zero line.

ducted earlier in our laboratory together with E.A. Burshtein demonstrated that the fluorescence quantum yield of the protein in RCs is approximately 0.02 [17]. This value is probably a consequence of efficient fluorescence quenching due to the excitation energy transfer to the porphyrin pigments of RCs, whose Soret absorption band overlaps the luminescence spectrum of tryptophan residues. Subunits L and M, associated with porphyrin and quinone cofactors of electron transfer in RC, contain 32 and 20 tryptophan residues, respectively [18]. Additional three tryptophan residues are localized in H-subunit of RC [19]. According to estimates made in [20], at least 20 tryptophan residues are located at a distance of approximately 20 Å from porphyrins, which is two times less than the Förster radius. Such a structural organization of RCs probably promotes effective energy migration from tryptophan residues to porphyrin pigments.

For the RCs dissolved in a 50% trehalose solution, the main peak of the fluorescence is shifted to the long-wave region (Fig. 3, curve 4), indicating increased mobility of the fluorophore environment. This fluorescence spectrum was also approximated well by two Gaussian curves:  $A1$  has a maximum at 329 nm with a half width of 37 nm, while  $A2$  has a maximum at 372 nm with a half width of 86 nm, dates not shown. The contribution of the second component increases relative to RCs in 70% glycerol solution by  $\approx 2.6$  times; the area ratio  $A2/A1 = 0.8$ . Both of these parameters reflect in particular that for the increased mobility of the protein as a whole and its peripheral areas.

Upon cooling of samples to  $-180^{\circ}\text{C}$  the tryptophan fluorescence maximum of RCs in glycerol is shifted to 322 nm and to 325 nm in trehalose, which is a consequence of the “freezing” of the fluorophore environment fluctuations at low temperatures. In the emission spectrum there are clearly visible the bands characteristic for phosphorescence of tryptophan occurred in the region of 400–500 nm (Fig. 3, curve 1). These bands were absent in the spectra at higher temperatures due to the very low quantum yield of the process. The position of the main fluorescence maximum was almost unchanged during heating of samples up to  $\sim -70^{\circ}\text{C}$  while the phosphorescence contribution dropped to zero (Fig. 3, curve 2). Upon a further temperature increase, a long-wavelength band (A2) is occurred in the fluorescence spectrum. The contribution of this band increased linearly with heating (the area ratio  $A2/A1$  depending on the temperature is shown in the insertion to Fig. 3). The maxima of the fluorescence spectra for the components A1 and A2 at temperatures above  $-70^{\circ}\text{C}$  were also almost linearly shifted toward longer wavelengths, indicating an increase in the dynamic activity of the chromophore environment. The dependence of the position maxima of two Gaussian components of the fluorescence spectrum of RCs in 70% glycerol on the temperature is shown in Fig. 4.

The temperature dependence of the micro-conformational dynamics of RC proteins also reflect the fluorescence lifetimes of tryptophan. In our experiments, the kinetics of tryptophan fluorescence decay of RCs was approximated with good fitting by the sum of two exponents. For the RCs in 70% glycerol at  $\lambda_{\text{reg}} = 325$  nm and temperature of  $20^{\circ}\text{C}$  the characteristic times were  $\tau_1 \approx 1.5$  ns and  $\tau_2 \approx 5.5$  ns, although earlier in these RCs at room temperature four components with durations of  $\approx 0.07$ , 0.5, 2, and 10 ns were detected [20]. The fastest components in [20] were attributed to the fluorescence of tryptophan residues located near porphyrin molecules in the RC structure. This a short time of the fluorescence is explained due to the energy migration to the porphyrin molecules by the Förster mechanism [20]. Long-lived nanosecond components were attributed by the authors to tryptophan residues of RCs situated in a more hydrophilic environment, e.g., closer to the surface of the protein globule. In this case the kinetic component with longer duration probably characterizes the emission of peripheral tryptophan residues and the kinetic component with short duration characterizes the emission of internal tryptophan residues. To a first approximation, they can be attributed to tryptophan residues of class II and class I.

The temperature dependences of  $\tau_{\text{av}}$  for RCs in 70% glycerol in samples frozen in the dark or in the light measured at wavelengths of 325 nm and 345 nm are shown in Fig. 5. Similar dependences of  $\tau_{\text{av}}$  versus temperature for RCs in trehalose are shown in Fig. 6.

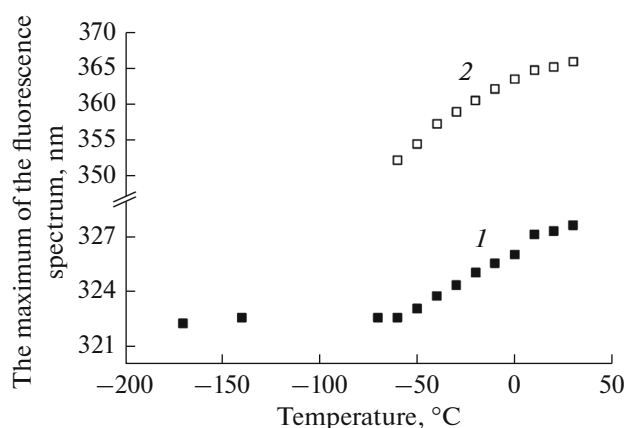


Fig. 4. The position of the maxima of two Gaussian components A1 (1) and A2 (2) of the fluorescence spectrum of RCs of *Rb. sphaeroides* in 70% glycerol versus temperature.

Obviously, the decrease of the duration of fluorescence with an increase in temperature reflects an increase in the mobility of the fluorophore environment [21]. We also see that when fluorescence was measured at higher wavelengths, a higher average duration was recorded. The same result was shown previously for RCs of *Rb. sphaeroides* at room temperature [20]. In addition, a similar increase in the duration of nanosecond fluorescence at the shift of the registration wavelength in the red area at room temperature was described in [22] for proteins with both internal and external tryptophan residues. It should be also noted that the duration of the fluorescence (units of nanoseconds) of pure tryptophan in an aqueous solution at room temperature increases with the increase of the registration wavelength, due to the contribution of different rotamers of the tryptophan molecule caused by various configurations of the alanyl side chain relative to the indole nucleus [23]. Transitions between these rotamers have an activation nature, including the participation of mobile protons of the nearest microenvironment, as shown by the isotope replacement of  $\text{D}_2\text{O} \rightarrow \text{H}_2\text{O}$ . A similar effect was observed for the water–glycerol (70%) solution of tryptophan in the entire temperature range from  $-180$  up to  $20^{\circ}\text{C}$  (data not shown).

As can be seen from Figs. 5 and 6, there is a marked difference in  $\tau_{\text{av}}$  values for RC samples cooled in the dark or in the activating light. On the other hand, in a dry RC film kept under atmospheric humidity such differences for freezing in the dark or in the light were not detected (data not shown). This effect is probably associated with the peculiarities of the intramolecular dynamics of the RC protein.

The comparison of the temperature dependences of the charge recombination rate in the RC structure (Figs. 1, 2) and the duration of the tryptophan fluorescence of the RC, reflecting the intramolecular dynamics of the RC protein (Figs. 5, 6)



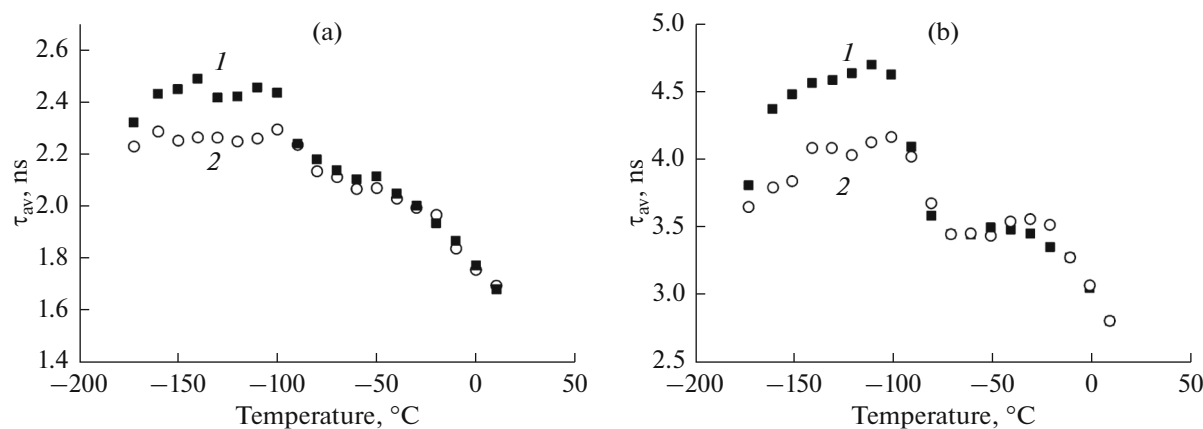


**Fig. 5.** The temperature dependences of average duration  $\tau_{av}$  fluorescence of tryptophan residues in RCs of *Rb. sphaeroides* in 70% glycerol, recorded at 325 nm (a) and 345 nm (b) during heating of RCs that were pre-frozen to  $-180^{\circ}\text{C}$  in the dark (1) and in the activating light (2). The accuracy of measurement of the lifetime  $\pm 0.05$  ns.  $\lambda_{ex} = 280$  nm.

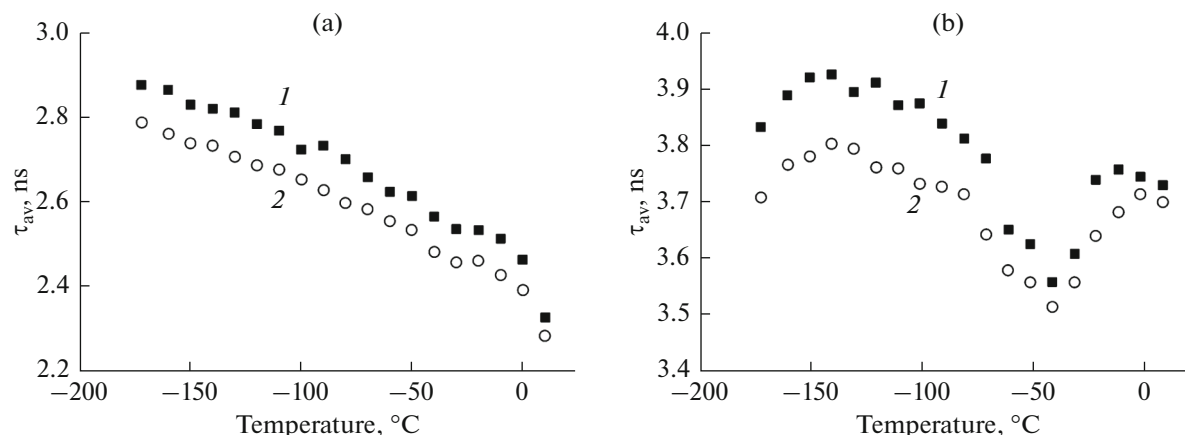


**Fig. 6.** The temperature dependences of the average duration  $\tau_{av}$  fluorescence of tryptophan residues in RCs of *Rb. sphaeroides* in trehalose, recorded at 325 nm (a) and 345 nm (b) during heating of RCs that were pre-frozen to  $-180^{\circ}\text{C}$  in the dark (1) and in the activating light (2). The accuracy of measurement of the lifetime  $\pm 0.05$  ns.  $\lambda_{ex} = 280$  nm.

demonstrated that the profiles of these changes in the  $-180 \dots \sim -80^{\circ}\text{C}$  temperature range coincide. When the RC was transferred to a trehalose environment, the temperature profiles of both functional and dynamic indicators were subjected to similar changes: in general, a flatter temperature dependence, an increase of the recombination rate constant at temperatures above  $\sim -50^{\circ}\text{C}$  ( $\lambda_{reg} = 600$  nm), was well correlated with the increase in  $\tau_{av}$  detected at 345 nm. It should be noted that changes in the duration of tryptophan fluorescence (Figs. 5, 6) were more expressed in the long wavelength region of the spectrum due to the increasing contribution of the second, slower component A2. Thus, at 325 nm, the contribution of A2 with an increase of temperature from  $-180^{\circ}\text{C}$  to room temperature rises from 0 to 15%, whereas at 345 nm it went from 0 to 23%. In general, the observed dependence of the average duration of fluorescence at different registration wavelengths was determined by both the actual

reduction in the lifetime of tryptophanys of classes I and II with increasing of the temperature and changes in their fluorescence spectra and the contributions of different fluorescent components. It should be noted that at cryogenic temperatures, the fluorescence spectrum of peripheral tryptophanys of class II is not different from the spectrum of internal tryptophanys of class I. This is shown by the good approximation of the entire spectrum with one Gaussian curve with a maximum at 322 nm. However, a second longwave Gaussian component A2 occurred at temperatures above  $-80^{\circ}\text{C}$ , which, upon further temperature increase of the conformational mobility of the environment increased its contribution and a shift toward the longer wavelengths area (Fig. 3). Such a change in the spectrum is superimposed on the changes of the lifetimes of the A1 and A2 components, leading to the appearance of nonmonotonic dependences of  $\tau_{av}$ , whose value fluctuates at different wavelengths due to differences in the

ratios of these components. As shown in Figs. 5a and 6a, for registration at 325 nm (which reflects the internal tryptophan of the RC) in this case  $\tau_{av}$  for the RCs in glycerol has smaller values than for RCs in trehalose. This effect is probably due to the higher mobility of the inner regions of the RCs in glycerol in comparison with RCs in trehalose. This may be due to a higher temperature of glass transition of samples in trehalose compared with the glycerol–water environment, resulting in higher inhibition of internal protein dynamics in the trehalose matrix at low temperatures [24]. According to [25, 26] the glass transition of the water–glycerol matrix occurs at  $\sim -120^\circ\text{C}$ . Different experimental methods indicate that activation of large-scale anharmonic activity in proteins, which is essential for their catalytic activity occurs during the heating of frozen sample to temperatures from approximately  $-90$  to  $-45^\circ\text{C}$ , the “global dynamic transition” range [27]. Nevertheless, enzymatic catalytic activity, which requires a corresponding intramolecular dynamics, can be observed at temperatures below this transition range [28, 29]. The presence of the conformational mobility changes of the protein that are sufficient for the enzymatic catalytic activity in the glass transition range was also observed by X-rays spectroscopy in [27].

However, when  $\tau_{av}$  was measured in the longer wavelength region of the spectrum (345 nm), values of  $\tau_{av}$  for RCs in the glycerol–water environment is higher than for RCs in trehalose (Figs. 5b and 6b). Consequently, there was a higher mobility of the surface area of the protein preserved in the trehalose environment, but not in the aqueous glycerol environment. In the presence of trehalose a specific change of the structural–dynamic state of the RC globule in comparison with glycerol probably occurs. The detailed mechanisms of the influence of the solvent environment on the conformational dynamics of the protein are still unknown [27]. There are certain assumptions about the interaction of trehalose with protein, resulting, in particular, in the known anti-denaturing stabilizing effect of this disaccharide. Some researchers believe that trehalose can replace hydration water molecules and form hydrogen bonds directly with the surface of the macromolecule [30, 31]. According to another hypothesis, trehalose does not directly bind with the surface of the macromolecule; however, it contributes to the retention of hydration water near the surface, which is accompanied by the formation of glasslike border structures between the macromolecule and the disaccharide [31, 32]. In such a case, water molecules in the surface regions of the protein preserve higher mobility [33]. The result is higher mobility in the surface regions of the protein surrounded by trehalose in comparison with the water–glycerol environment.

The comparison of the temperature dependences of the recombination rate of separated charges in RCs

frozen in the dark and in the light in different solvents (Figs. 1, 2) and the internal dynamics of RCs reflected by fluorescent indicators under similar conditions (Figs. 3–6), showed that processes of the stabilization of charges separated between the bacteriochlorophyll dimer and the quinone acceptor is affected by the structural and functional properties of the entire protein globule. The ion-radical pair  $\text{P870}^+\text{Q}_\text{A}^-$  is the source of a strong electric field, which affects the charged groups of the protein, changing their spatial orientation. Indirectly this effect is manifested in the fluorescence characteristics of the tryptophan residues. In this case, the inner fluorescent indicators probably mainly reflect the situation in the quinone acceptor part of an RC, since almost half of the tryptophan of an RC are located at very small distances from the photoactive pigment of the RC and  $\text{Q}_\text{A}$  and  $\text{Q}_\text{B}$  quinones. So we determined a generalized mechanism for the stabilization of separated charges in an RC that corresponds to the known experimental observations. According to these observations, efficient electrostatic stabilization of an electron on the  $\text{Q}_\text{A}$  and  $\text{Q}_\text{B}$  quinone acceptors is associated with displacements of protons in their protein environment; it involves not only the protonated amino-acid residues of the nearest environment of quinone cofactors in these processes. In particular, it was shown that the change in the charge state of quinones is accompanied by changes of the  $pK$  of protonatable amino acids at distances up to  $15\text{--}17\text{ \AA}$  [34–36], while the rate of dark charge recombination also depends on the condition and composition of the lipid environment of an RC [37, 38].

It is also interesting to note that for cooling in the light, lower fluorescence lifetimes of tryptophans (in condition where there is a difference) than for cooling in the dark were recorded. This corresponds to changes in a functional indicator: in RCs cooled in the light, the recombination rate constant for charges divided between  $\text{P}^+$  and  $\text{Q}_\text{A}^-$  is close to that for those at room temperature, in contrast to the situation with cooling in the dark.

Based on these results it can be assumed that RCs exist in two main macroconformations: “fast” and “slow,” which are characterized by different rates of the  $\text{P}^+$  and  $\text{Q}_\text{A}^-$  recombination reaction. The “fast” (or dark-adapted) conformation of RCs, when  $\text{Q}_\text{A}$  is ready to accept an electron from P, freezes under cooling in the dark; however,  $\text{Q}_\text{A}$  is not reduced under these conditions. “Slow” (light-adapted) conformation of RC occurs and is fixed when  $\text{Q}_\text{A}$  is reduced under light conditions during freezing. Transitions can occur between these states, the rate of transitions increases with increasing temperature. Simultaneously with the total conformational relaxation of RCs that accompanies electron transfer, local relaxation of the hydrogen bonds formed by  $\text{Q}_\text{A}$  with the surrounding protein

occurs. As was shown in [39, 40], the mechanism of proton relaxation of hydrogen bonds during reduction of  $Q_A$  is responsible for the anomalous temperature dependence of the recombination rate constants (it decreases with increasing temperature) for RCs that were frozen in the dark. This proton relaxation is due to a change in the occupation (the probability of localization) of protons in the double-well potential of the hydrogen bond, which occurs as the result of the reduction of  $Q_A$ . It is important that the rate of the proton relaxation decreases with increasing temperature, while the rate of activation relaxation, conversely, increases with increasing temperature. The observed temperature dependence of the recombination rate constant for RCs frozen in the light may be qualitatively explained by the consequence of the simultaneous action of two competing processes: activation of the transition between the “slow” and “fast” conformations of RCs that are occupied in the light. This transition accelerates with increasing temperature and the overall rate of the recombination reaction (the peak at  $-110^\circ\text{C}$ ) and proton relaxation in the structure of the hydrogen bonds of the local environment of  $Q_A$ , which slows with increasing temperature and decreases the recombination rate constant. Modification of the intramolecular dynamics, as reflected by the temperature dependences of the fluorescent indicator when glycerol in the environment of the RC is replaced by trehalose transforms the temperature profiles of the recombination rate. A “shallower” temperature dependence of the recombination rate constant in samples frozen in the dark was observed; the maximum at  $-110^\circ\text{C}$  disappeared in RCs frozen in the light and it decreased further at a temperature of  $\sim -40^\circ\text{C}$  with a consequent increase to room temperatures.

## ACKNOWLEDGMENTS

The authors are grateful to the Russian Foundation for Basic Research (projects no. 14-04-01536, 15-29-01167) for partial financial support of this study.

## REFERENCES

1. A. M. Streltsov, A. G. Yakovlev, A. Ya. Shkuropatov, et al. *FEBS Lett.* **357**, 239 (1995).
2. V. Z. Paschenko, V. V. Gorokhov, N. P. Grishanova, et al., *Biochim. Biophys. Acta* **1364**, 361 (1998).
3. A. A. Kononenko, P. P. Knox, S. K. Chamorovskii, et al., *Khim. Fizika* **5**, 795 (1986).
4. G. A. Abgaryan, L. N. Christoprov, A. O. Goushcha, et al., *J. Biol. Phys.* **24**, 1 (1998).
5. B. H. McMahon, J. D. Muller, C. A. Wright, and G. U. Nienhaus, *Biophys. J.* **74**, 2567 (1998).
6. P. Maroti, and C. A. Wraight, *Biophys. J.* **73**, 367 (1997).
7. P. P. Knox, P. M. Krasilnikov, E. P. Lukashev, et al., *Dokl. Biochem. Biophys. Nauk* **455**, 49 (2014).
8. P. P. Knox, E. P. Lukashev, A. A. Kononenko, et al., *Mol. Biol. (Moscow)* **11**, 1090 (1977).
9. Y. Chen and M. D. Barkley, *Biochemistry* **3**, 9976 (1998).
10. E. A. Burshtein, *Mol. Biol. (Moscow)* **17**, 455 (1983).
11. J. R. Albani, *J. Fluoresc.* **21**, 1301 (2011).
12. N. I. Zakharova and I. Yu. Churbanova, *Biochemistry (Moscow)* **65** (2), 149 (2000).
13. P. P. Knox, V. V. Gorokhov, and V. Z. Pashchenko, in *Current Problems of Photosynthesis*, Ed. by S. I. Alakhverdiev, A. B. Rubin, and V. A. Shuvalov (Moscow—Izhevsk, 2014), **Vol. 1**, pp. 225–268 [in Russian].
14. G. Palazzo, A. Mallardi, A. Hochkoepler, et al., *Biophys. J.* **82**, 558 (2002).
15. Y. K. Reshetnyak and E. A. Burstein, *Biophys. J.* **81**, 1710 (2001).
16. S. V. Konev and I. D. Volotovskii, *Photobiology (Beloruss. State Univ., Minsk, 1979)* [in Russian].
17. N. I. Zakharova, E. A. Permyakov, M. Fabian, et al., *Mol. Biol. (Moscow)* **18** (3), 719 (1984).
18. J. C. Williams, L. A. Steiner, G. Feher, and M. I. Simon, *Proc. Natl. Acad. Sci. U. S. A.* **81**, 7303 (1984).
19. I. Fathir, T. Mori, T. Nogi, et al., *Eur. J. Biochem.* **268**, 2652 (2001).
20. V. I. Godik, R. E. Blankenship, T. P. Causgrove, and N. Woodbury, *FEBS Lett.* **321**, 229 (1993).
21. J. R. Alcala, E. Gratton, and F. G. Prendergast, *Biophys. J.* **51**, 925 (1987).
22. J. R. Albani, *J. Fluoresc.* **21**, 1301 (2011).
23. A. G. Szabo and D. M. Rayner, *J. Am. Chem. Soc.* **102**, 554 (1980).
24. P. D. Miller, J. J. de Pablo, and H. R. Corti, *J. Phys. Chem. B* **103**, 10243 (1999).
25. W. W. Wright, G. T. Guffanti, and J. M. Vanderkooi, *Biophys. J.* **85**, 1980 (2003).
26. J. L. Dashnau, B. Zelent, and J. M. Vanderkooi, *Biophys. Chem.* **114**, 71 (2005).
27. M. Weik, R. B. G. Ravelli, I. Silman, et al., *Prot. Sci.* **10**, 1953 (2001).
28. N. More, R. M. Daniel, and H. H. Petach, *Biochem. J.* **305**, 17 (1995).
29. R. M. Daniel, J. C. Smith, M. Ferrand, et al., *Biophys. J.* **75**, 2504 (1998).
30. J. F. Carpenter and J. H. Crowe, *Biochemistry* **28**, 3916 (1989).
31. S. Paul and S. Paul, *J. Phys. Chem. B* **119**, 1598 (2015).
32. P. S. Belton and A. M. Gil, *Biopolymers* **34**, 957 (1994).
33. J. Schlichter, J. Friedrich, L. Herenyi, and J. Fidy, *Biophys. J.* **80**, 2011 (2001).
34. M. Y. Okamura and G. Feher, *Annu. Rev. Biochem.* **61**, 861 (1992).
35. C. R. D. Lancaster, H. Michel, B. Honig, and M. R. Gunner, *Biophys. J.* **70**, 2469 (1996).
36. J. Miksovska, P. Maroti, J. Tandori, et al., *Biochemistry* **35**, 15411 (1996).
37. P. Maroti, *J. Photochem. Photobiol. B* **8**, 263 (1991).
38. J. Lavergne, C. Matthews, and N. Ginet, *Biochemistry* **38**, 4542 (1999).
39. P. M. Krasilnikov, P. A. Mamonov, P. P. Knox, et al., *Biochim. Biophys. Acta* **1767**, 541 (2007).
40. P. M. Krasilnikov, P. P. Knox, and A. B. Rubin, *Photochem. Photobiol. Sci.* **8**, 181 (2009).

Translated by V. Mittova